2018

Air-sea coupling dependency on sea surface temperature fronts as observed by research vessel data.

Catherine L. Stauffer

THE FLORIDA STATE UNIVERSITY

COLLEGE OF ARTS AND SCIENCES

AIR-SEA COUPLING DEPENDENCY ON SEA SURFACE TEMPERATURE FRONTS AS OBSERVED BY RESEARCH VESSEL DATA

By

CATHERINE L. STAUFFER

A Thesis submitted to the
Department of Earth, Ocean and Atmospheric Sciences
in partial fulfillment of the requirements for graduation with
Honors in the Major

Degree Awarded:
Spring 2018

The members of the Defense Committee approve the thesis of Catherine L. Stauffer defended on 26 March 2018.

Mark A. Bourassa

Dr. Mark Bourassa
Thesis Director

Dr. Jerry Magnan
Outside Committee Member

Dr. Zhaohua Wu
Committee Member

Table of Contents

Abstract 4

1 Introduction 5

2 Background 5

3 Objectives 8

4 Methodology and Data 9

5 Results 14

6 Conclusions 19

Abstract

A better understanding of the driving mechanism behind the atmospheric response to a sea surface temperature front is essential for numerical weather prediction models to accurately resolve the relationship. This study uses a novel approach, supported by in situ observations, to investigate the two most commonly proposed driving mechanisms – changing pressure and changing stability. Atmospheric response to sea surface temperature fronts is examined using high resolution research vessel data. Using the recorded meteorological and oceanographic observations and a bulk flux testbed, the behavior of decreased stability and increased winds going from cold to warm waters is found to be consistent with previous analyses of the air-sea coupled system. Furthermore, it is revealed that stability and pressure changes occur simultaneously with or before atmospheric temperature responses to sea surface temperature fronts. This suggests that both mechanisms play an important role in the atmospheric temperature response.

1 Introduction

The subject of air-sea coupling (interaction between the ocean and the atmosphere) is an increasingly studied field, as its use in climate and weather prediction models has amplified over the years. Specifically, the dominant physical processes driving the evolution of this coupled air-sea system over sea surface temperature (SST) fronts is an ardently discussed topic of interest. The processes that transfer momentum, energy, moisture, and matter through the ocean surface are key to ocean climate and weather, and they are closely linked to air-sea interaction. These processes affect ocean circulation, global water supply, and the influence of the ocean on the atmosphere and vice-versa. This study uses research vessel (RV) data to interpret the changes in atmospheric properties and the driving air-sea coupling fluxes involved in the evolution of the atmosphere related to the passage of air over SST fronts. This study provides a new approach and further insight into the debate over what drives the atmospheric response to an SST front: a perturbed pressure gradient or instability.

2 Background

The primary mechanism by which SST-induced changes occur is heavily debated. Extensive work has been conducted in this area with respect to surface wind and wind stress response over SST fronts, as outlined by Hughes (2014). Common contributors to increased surface wind speeds over warm waters are summarized by Small et al. (2008), O'Neill (2012), and Hughes (2014).

Two different explanations have emerged as the most popular among researchers seeking to identify the primary mechanism that drives the atmospheric response to an SST front. The first explanation is an increased pressure gradient force caused by atmospheric baroclinicity for

systems moving from cool to warm waters (and vice versa), as demonstrated by Song et al. (2006) and Small et al. (2003).

The other mechanism often proposed is based on the instability of the atmospheric boundary-layer. This was demonstrated by Hayes et al. (1989) using a phase analysis of the wind speeds and SST. Wallace et al. (1989) and Hayes et al. (1989) outlined additional studies that favor the instability of the boundary-layer on the warmer side of SST fronts, thus emphasizing the resultant increase in downward mixing of momentum. This mixing increases the surface winds due to the reduced stability over the warm waters (Tokinaga et al. 2005). Both Small et al. (2003) and Hughes (2014) concluded that baroclinicity was the driving mechanism of the coupled system; however, both studies acknowledged that the stability-related process cannot be ruled out on smaller spatial scales and as contributors to the changes in surface wind.

Spall (2007) used idealized model cases to find consistent reports that there is an acceleration in wind speeds over the warm waters of SST fronts. However, the study found that the acceleration of the winds was caused by an imbalance in the Coriolis Force associated with rapid turbulent mixing and vertical transport of winds, rather than the aforementioned mixing of momentum and adjustment pressure gradient force.

Small et al. (2008) outlined the known reasons for atmospheric dependency on SST fronts. These include: changes in stability, stress, latent heat, and sensible heat fluxes; the potential effect of a pressure gradient resulting from atmospheric responses to changing fluxes on atmospheric circulation; and the transport of moisture and momentum through the atmosphere. Small emphasized that the importance of the moisture and energy transfer is still unknown.

A better understanding of the driving mechanism behind the atmospheric response to an SST front, supported by satellite and in situ observations, is essential for numerical weather prediction models to accurately resolve the relationship. Chelton (2004) used a parameterization of a previously observed relationship between SST gradients and the curl of stress demonstrated in multiple studies (e.g. Sweet et al. (1981), Jury and Walker (1988), Wallace et al. (1989), and Hayes et al. (1989)) to investigate the importance of SST parameterization in numerical weather prediction models. Chelton and others found that low-level winds were strongly influenced by the presence of an SST front (e.g., in various ocean basins such as the Gulf Stream and eastern tropical Pacific and by various platforms including satellite, aircraft, and ship observations). Expanding upon this work, Chelton used the results from these observational studies as a standard for comparison to examine how changes (made in 2001) to the European Centre for Medium-Range Weather Forecasts (ECMWF) model changed in its representation of SST-related wind variability. Chelton concluded that modeling the lower atmosphere and the ocean benefited greatly from the higher resolution SST boundary condition specification improvement to the ECMWF model.

The air-sea temperature differences related to the two explanations most often put forth in previous studies assume that either (1) the air temperature responds very slowly to changes in SST, or (2) the air temperature responds very rapidly to changes in SST. However, these cases asymptote to two extremes: (1) the atmosphere is thermodynamically non-response to the ocean on these scales studies (less than 1000km), or (2) that the changes in the ocean are matched by changes in the atmosphere, with negligible delay. Thus, this study observes high resolution SST and air temperature in order to gain greater insight into the dominant coupling mechanism. It also seeks to analyze the changing turbulent fluxes, those known to adjust to SST gradients (e.g.,

momentum) and those that have more speculative responses, that would influence changes to the atmosphere (e.g. sensible and latent heat fluxes). These investigations use RV data and a turbulent flux model to examine the changes associated with several gradients.

3 Objectives

The in situ observations used are from RV data accessed from the Shipboard Automated Meteorological and Oceanographic System (SAMOS) database to study the atmospheric response to SST fronts (see section 4.5 Data for more information on the datasets). SST fronts are found by plotting the observed SSTs with respect to time in order to find temperature gradients in the data. Gradients are determined by distinct increases (or decreases) from one general average temperature to another. The specific objectives are as follows:

1. Determine how much the anemometer winds change in association with changing SST values. This is achieved by plotting the marine meteorological data of select RV missions with respect to time and by identifying changes or patterns in the wind before and after the observed SST front. The change in the associated air-sea fluxes are then investigated. These fluxes are not measured on most RVs; therefore, they are calculated through bulk formulas (Bourassa et al. 1999 and references therein; Moroni 2008) and recorded for the various RV cruises being studied.
2. Explore how air temperature is affected by SST to determine the dominant coupling mechanism, as previously discussed. If the air temperature rapidly responds to the SST front, we look for a pressure gradient dependence on air temperature. If it is not totally dependent upon the SST front, we explore the changes in air-sea temperature differences and how stratification influences winds and fluxes. These analyses are conducted by

plotting the SST and air temperature with respect to time and by identifying patterns in the air response before and after the SST front. It is possible that both processes come into play and that each dominates for distance or a time scale that might be identifiable from the RV observations.

4 Methodology and Data

An analysis of the response of the atmosphere is made based on plots of the air and sea temperature and wind speed and direction with respect to time. Different combinations of wind direction and SST gradients characterize the air-sea temperature differences and fluxes.

Since it is possible that an RV is not always headed in the same direction as the wind, each non-SST and wind plot is adjusted to standardize the way the coupled system is viewed. This process is explained further in section 4.3 Wind Speed and Direction.

4.1 Sea Surface Temperature Fronts

Each RV mission's SSTs are plotted with respect to time in order to identify the fronts to be studied. These fronts are denoted by a significant gradient displayed in the SST plots. **Figure 1** shows a small SST gradient from minute to around minute 70. Through this process, 57 SST fronts are identified and then trimmed down to the 31 cases being studied based on quality of the rest of the observation data.

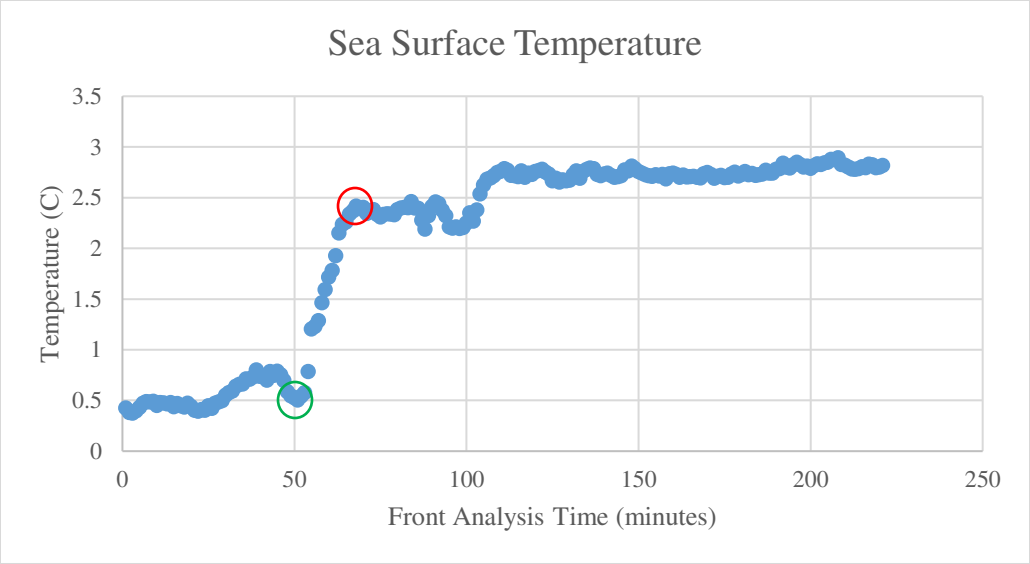

Figure 1 shows an example of a SST-front found from the KCEJ 20071017 cruise. The start time is around minute 50 (green circle), where the SST goes from a general average state to a sharp increase. The end time is around minute 70 (red circle), when the sharp gradient ceases and the SST goes back to a general average state again. This would be an up-gradient example since the SST goes from cooler temperatures to warmer after the largest gradient (minute 50-70).

4.2 Air Temperature Response

Figure 2 shows that as the front proceeds there is a delay in the atmospheric temperature changes, suggesting that while the air mass responds and changes due to the presence of the front, it does not respond immediately. This is consistent with findings in previous studies (e.g., Sweet et al., 1981) and points to mechanisms for which the air temperature responds to changes in SST.

Air temperature is analyzed in this manner for each RV cruise dataset used in this study. The rapidness of the response to changes in SST is examined in (section 5.2 Air Temperature Response). The associated fluxes are a critical element and key to understanding the governing processes of the SST-induced interaction of the ocean and air.

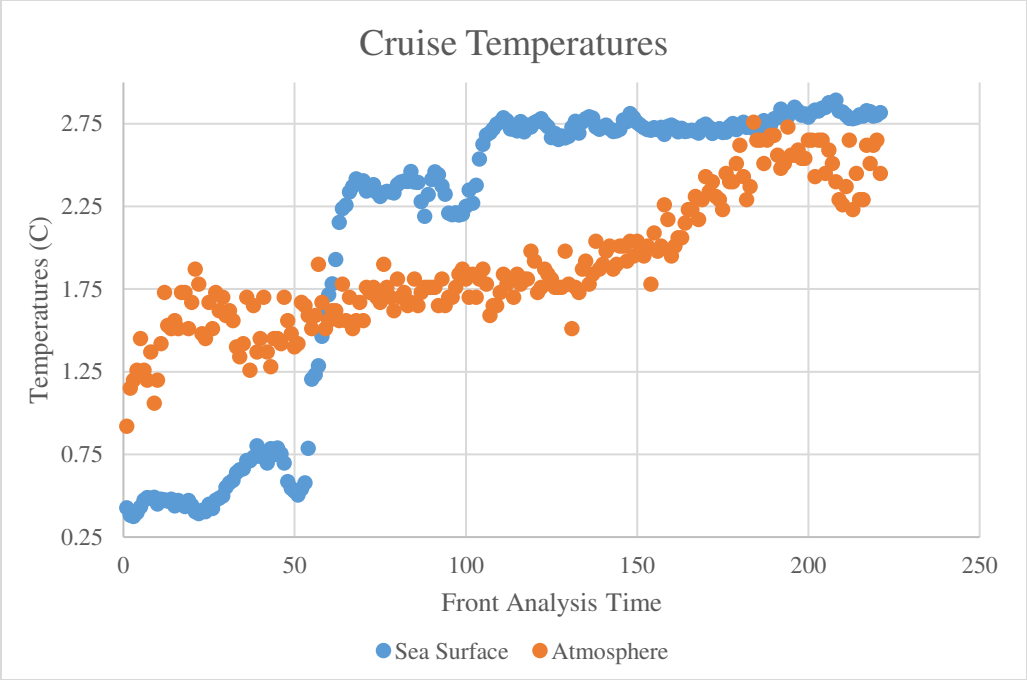

Figure 2 shows the KCEJ 20071017 cruise. Plotted are the sea surface and atmospheric temperatures.

4.3 Wind Speed and Direction

Wind speeds and directions are analyzed in a similar manner as the air temperature response (4.2). The time series from both sets of observations are plotted to characterize patterns in the change as associated with the SST front.

Each front is categorized based upon the temperature change of the waters. In order to standardize the method in which the SST-related response is analyzed, it is imperative that the front be categorized based on wind direction rather than the direction of ship's passage. The wind barbs and motion vector of the RV platform are plotted in their place on a latitude-longitude grid to check for opposing directions, **Figure 3**. If the directions are opposing, the data timeseries without standardization is going in the opposite direction to that of the wind. Since it cannot be looked at chronologically, the atmospheric response is inspected upstream, which is to

say in reverse. So, when looking from left to right at any plot for a given cruise, the data are presented in the direction relative to the wind.

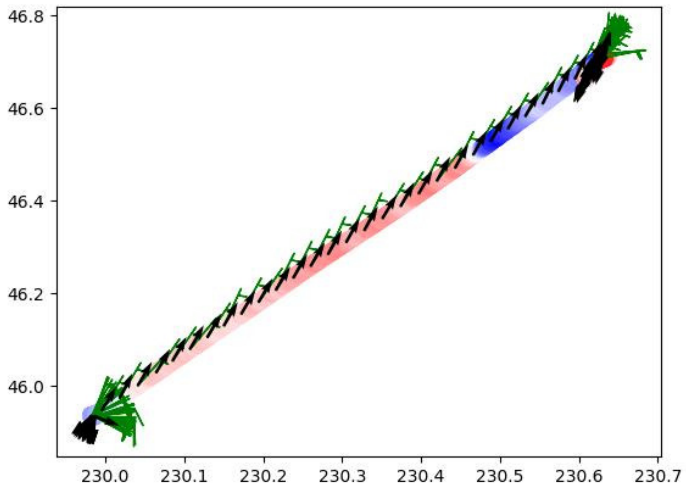

Figure 3 is a scatter plot of the SST values (colored dots), wind barbs, and motion vectors of the ship plotted on a latitude/longitude grid for the RV cruise KAQP20070817. For this cruise, the whole path travelled of the RV is in the opposite direction than that of the wind. This would be a case where the atmospheric response would be looked at in reverse-order because the ship is measuring the response before it measures passes the front.

4.4 Calculation of Fluxes

The boundary-layer model of the Modularized Flux Testbed (MFT) uses known values of wind speeds, potential temperatures, and humidities to simultaneously calculate height adjusted to 10 meters and the turbulent fluxes (latent heat flux, sensible heat flux and stress) associated with the air-sea coupling. These fluxes apply selected parameterizations (based on the limitations of the available data and model concepts) compiled from various models described in Moroni (2008). The MFT is designed in such a way as to control which of the parameters change and which are held constant (Moroni, 2008). The MFT provides a wide selection of flux-related parameterizations to choose from. This study uses the roughness length parameterization for momentum by Bourassa (2006) and the roughness length parameterization for potential

temperature and moisture by Clayson, Fairall, and Curry (1996). These parameterizations are well suited for this study because the RV data do not include wave data; thus, the winds and waves will be assumed as in local equilibrium, limiting the model selection and forcing several parameters to be constant.

The resultant fluxes cover various hypotheses of the governing physical mechanism presented by earlier work, outlined in Small et al. (2008). What makes this study unique is the sole use of in situ RV data, instead of satellite and numerical model simulations, and the calculation of the fluxes describing the known changes of the corresponding pressure gradient. The spatial resolution of these observations is also novel, revealing the rate at which air temperature responds to SST, which, as stated previously, is related to the surface energy fluxes. While the values of the turbulent fluxes (sensible and latent heat fluxes) are dependent on the parameterization, modern parameterizations will rarely lead to large differences in values for the environments that are being examined.

4.5 Data

The datasets used are collections of 1-minute average navigational, meteorological, and oceanographic observations from select research vessels collected by the SAMOS initiative. Of the numerous observations collected by the RVs, this study makes use of the air and sea temperature, wind speed and direction, and pressure data.

5 Results

5.1 Wind Response

As described in Section 2, an acceleration of wind speeds from cold to warm waters is expected along with a deceleration of wind speeds from warm to cold waters. We define SST fronts that go from cold to warm waters as "up-gradient fronts" (UGs) and those that go from warm to cold waters as "down-gradient fronts" (DGs).

The table below outlines the acceleration and deceleration cases associated with each gradient type.

	Accelerates	Decelerates
Up-gradient	10	5
Down-gradient	4	12

Table 1 displays the 31 fronts selected for study studied based on quality of the observation data. These are divided based on the direction of the gradient and the wind speed response to the front.

71% of the UG cases and 71% of the DG cases follow the above theory of wind speeds increasing and decreasing, respectively, as they cross the front. Most of the cases (71%) follow the theory provided. The wind speeds' pattern of variability and adjustment tends to follow the curve of the air temperature variability and change. The main speed adjustment occurs where the difference in SST and the temperature of the atmosphere (SST-TA) is at a local maximum or minimum.

	Counterclockwise	**Clockwise**	**Steady**
Up-gradient	10	4	4
Down-gradient	4	6	3

Table 2 displays the 31 fronts divided based on the direction of the gradient and the wind direction change before the front.

The response of the wind direction is more variable and less defined than that of the speeds. **Table 2** shows that the wind mostly turns clockwise (46%) before the front in DG cases and counterclockwise (56%) before the front in UG cases. Future work could involve an in-depth analysis of the rotation of the wind across the front and any affect it may have on the atmospheric response.

5.2 Atmospheric Temperature Response

When analyzing the time for the atmospheric temperature to adjust after a front starts, cases are split into four categories: quick, neutral, slow, and before. A "quick" response is defined as the atmospheric temperature starting a distinct gradient within zero to five minutes after the start of the SST gradient. A "neutral" response is defined as a five- to 15-minute response time, and a "slow" response is a response time greater than 15 minutes.

Cases categorized as having a "before" response are those where the atmosphere is already changing by the start of the SST front. Five of the 31 cases used in this study show an atmospheric temperature change well before the start of the gradient. Only the 26 cases with an atmospheric response at or after the start of the front are analyzed. **Table 3** shows the distribution of the response times of the datasets analyzed.

	Up-Gradient	**Down-Gradient**
Fast Response	4	5
Neutral Response	5	5
Slow Response	4	3

Table 3 shows the number of cases of the style of front (up- or down-gradient).

This result is interesting as there is no clear dominating mechanism, the response times for each gradient type have an equal distribution.

5.2.1 Quick Response

The nine cases in which the atmosphere reacts quickly to the SST front leads to an exploration of the response of the pressure in this coupled system. As shown in **Table 4**, the pressure changes within 10 minutes of the start of the SST front. The pressure response time is split evenly between changing simultaneously with the atmospheric temperature and starting five minutes after the atmosphere has started changing. **Table 4** shows the rest of the distribution of pressure response times to the atmospheric temperature response times as defined in Section 5.2.

	0 - 5 min	5 - 10 min	10+ min
Quick Response	5	4	0
Slow Response	3	0	4
Neutral Response	4	5	1

Table 4 displays the response time of the change in pressure to the SST front for each atmospheric response type. Here Quick, Slow, and Neutral refer to the atmospheric temperature response time described in Section 5.2. The times are how long it to the pressure to adjust to the front.

5.2.2 Slow Response

For slow-response fronts, the focus is on analysis of the effect of SST-TA on the winds and fluxes with an emphasis on stability before and after the front.

The SST fronts have a general start time and end time, as shown in **Figure 2**. When plotting an SST-TA, the start of the gradient and the SST are simultaneous. The end of the SST-TA gradient also occurs simultaneously with that of the SST. This is expected since the SST-TA is simply the difference between SST and atmospheric temperature, making it an adjusted SST gradient.

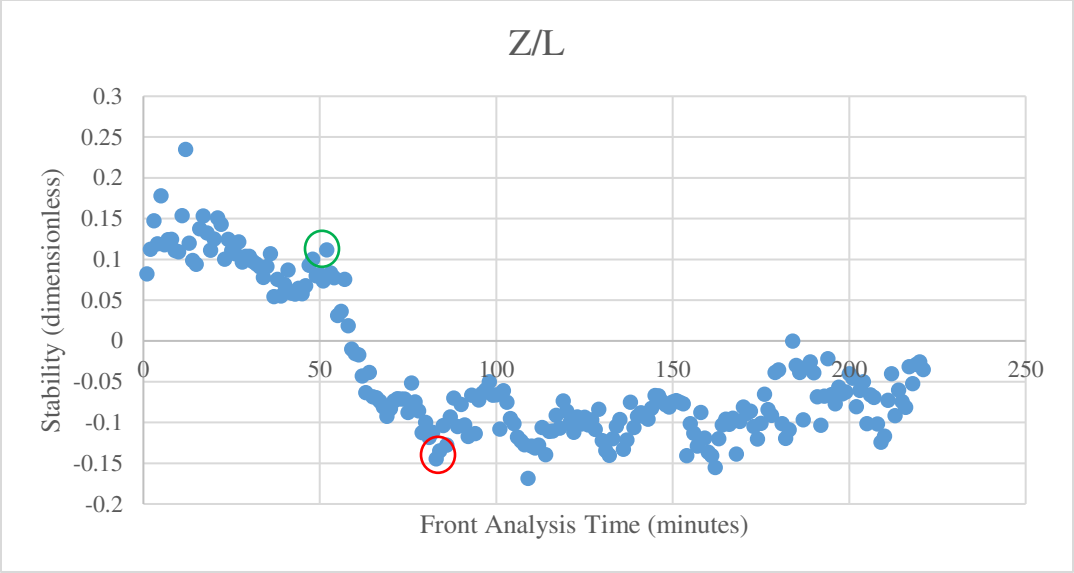

Figure 4 shows an example of the calculated stability (dimensionless Monin-Obuhkoy stability) from the KCEJ 20071017 cruise. Time corresponds to that shown in **Figure 1**. The start and end time of the stability gradient is around that of the SST gradient, minute 50-70. As the SST goes from colder waters to warmer, the environment goes from being stable (positive values) to unstable (negative values).

The stability, as measured by a dimensionless Monin-Obuhkov scale (M-O parameter) also adjusts from one general average to a new general average during passage over the SST front, as depicted in **Figure 4**. Whether the M-O parameter becomes more stable or less stable is dependent on the direction of the gradient relative to the direction the wind is moving. Consistent with previously discussed theory, all of the UG cases are unstable after the gradient. As for the DG cases, two of the three slow response DG were stable making the majority consistent with previous findings. The winds start to react strongly to the gradients at the peak of the SST-TA gradient and at the bottom of the stability gradient, near where the change in stability bottoms out.

As shown in **Figure 5,** the stability adjusts back to pre-SST front values where the SST-TA gradient ceases but the heat fluxes and stress adjusts to a new general average different than that of the pre-SST front.

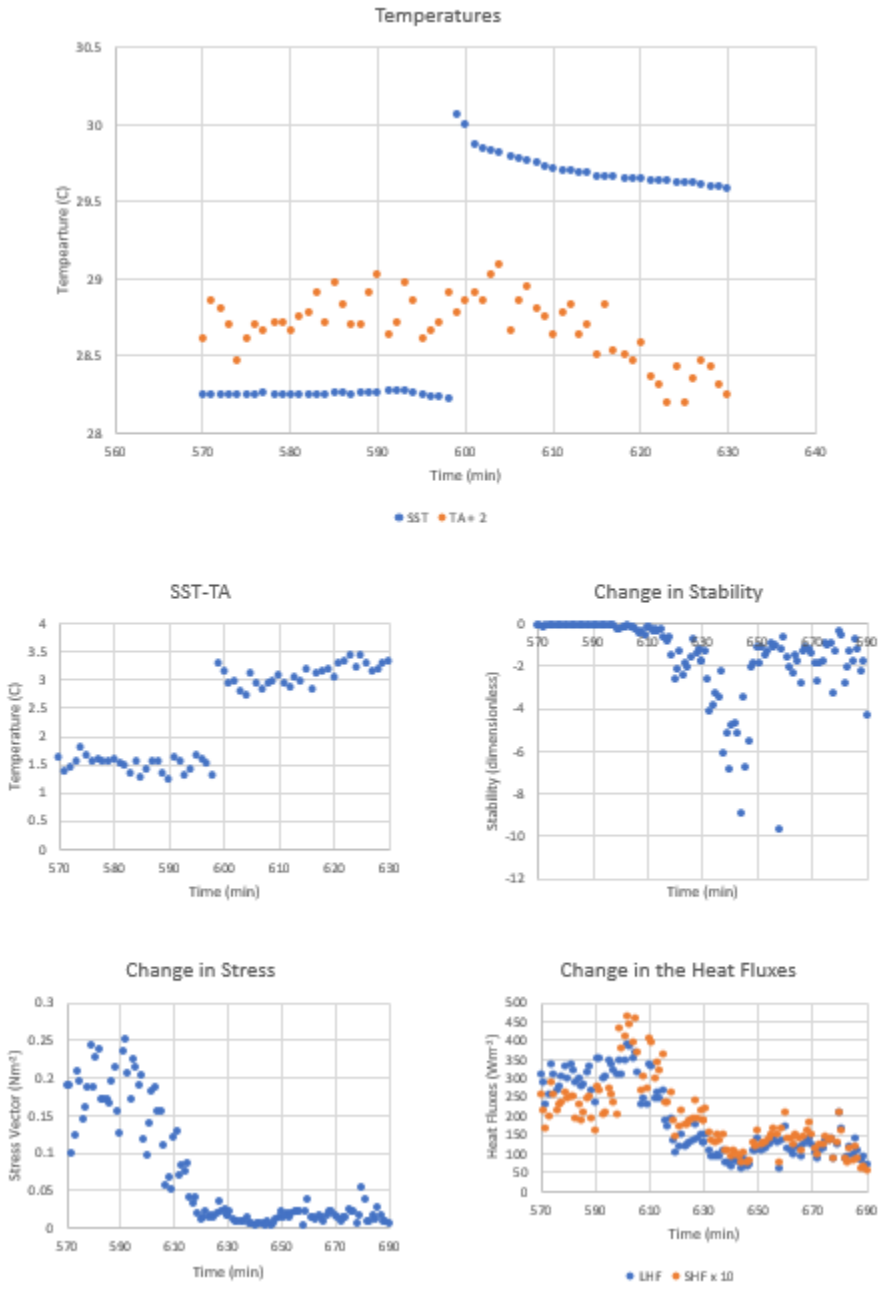

Figure 5 shows an example of all the conditions analyzed in this study from the KCEJ 20071228 cruise. The graphic on the left shows the SST in blue and the atmospheric temperature in orange. In this example the atmospheric temperature responds to the gradient within four or five minutes. The cluster of four graphics to the right are, starting at the top left and moving clockwise, as follows: the SST-TA difference, change in stability, change in stress, and change in the heat fluxes (where latent heat flux is in blue and sensible heat flux is in orange). This example shows clearly the stability starting its dramatic change at the top of the SST-TA gradient. Around the top of the SST-TA gradient is also where the stress and heat fluxes steady out to their new general average.

5.2.3 Neutral Response

	Stable	Unstable
0-5 min	3	1
5-10 min	2	3
10+min	1	0

Table 5 shows associated stability with each pressure response time of the neutral cases.

As **Table 3** depicts, the UG cases primarily become unstable at the start of the front while DG cases primarily become stable. However, for these neutral cases, there are more outliers than the other two cases. When looking at stability versus pressure response time (**Figure 5**), the less than five minutes pressure response times favor stable frontal conditions. Other than that distinction, the spread in response time is decently even.

The pressure responds simultaneously with or before the atmosphere responds to the SST front for every neutral cruise save one. This, paired with the stability patterns starting with the SST front like the slow response time (5.2.2), suggests that the changing pressure over the front is a means by which the atmosphere responds to the front. However, the stability consistently changes for all 31 cases as soon as the SST changes. Using the same reasoning as the changing pressure, the changing stability over the front is also a means by which the atmosphere responds to the front.

6 Conclusions

There are two main approaches to determining the governing mechanism of a coupled air-sea system passing over an SST front this study utilizes: changes in pressure gradient and stability. As presented in Section 3, we consider that both may play an important role. The approach is to

use in situ data rather than satellite data or numerical weather prediction models, both of which have trouble resolving small spatial scale (less than 50km) changes in features.

Analyzing the evolution of the wind speed as it passes over an SST front produces results consistent with previous studies. The winds speed up as the SST goes from cold to warm water and slow down as the SST goes from warm to cold water. The atmosphere becomes unstable as the SST goes from cold to warm and stable as the SST goes from warm to cold waters. Additionally, the stability dramatically decreases over warmer waters during the SST event and while the atmospheric temperature adjusts to the front. However, eventually the stability returns to its pre-SST state. The heat fluxes and momentum then start responding after the stability and SST gradients return to near zero values. The timing of the stability change relative to the atmospheric temperature and flux change suggests it being a method by which the atmospheric winds and temperature adjusts.

Although pressure adjustments are relatively small and less dramatic than the temperatures, the timing of the pressure change suggests a primary influence on the atmospheric response. Most of the pressure response times occurred before or simultaneously with the atmospheric response.

6.1 Future Work

As discussed in 5.2, there was an even distribution of response times to gradient type. This is an unexpected result, as it suggests there is no dominating mechanism in atmospheric response to SST gradients. Looking further into how the difference between SST and air temperature evolves over the SST front, as opposed to solely the air temperature, may result in a more distinct dominating response.

This study analyzed the data temporally. However, because the ocean, ship, and winds are all moving in different directions at different rates, analyzing the data as spatially might contain different results. The data can be analyzed as a function of how far the ship is from the front versus how much time has passed before and after the front.

Similarly, there are two metrics by which the data can be analyzed. One is sorting the results by the dot product of the wind vector and the SST gradient the other by wind speed (Nicklaus Schneider, personal communication, 2018). The first metric mentioned would replace the up-gradient and down-gradient style used in this study.

References

Bourassa, M. A. (2006). Satellite-based observations of surface turbulent stress during severe weather. W. Atmosphere - Ocean Interactions, 2, pp. 35 - 52. doi:10.2495/978-1-85312-929-2/02

Bourassa, M. A., Vincent, D. G., Wood, W. L. (1999), A flux parameterization including the effects of capillary waves and sea state. Journal of Atmospheric Science, 56, 1123-1139. doi:10.1175/1520-0469(1999)056%3C1123:AFPITE%3E2.0.CO;2

Chelton, D.B. (2005), The impact of SST specification on ECMWF surface wind stress fields in the Eastern Tropical Pacific. Journal of Climate, 18, 530–550. doi:10.1175/JCLI-3275.1

Clayson, C. A., C. W. Fairall, and J. A. Curry, 1996: Evaluation of turbulent fluxes at the ocean surface using surface renewal theory. J. Geophys. Res., **101**, 28503□28513

Hayes, S. P., McPhaden, M. J., & Wallace, J. M. (1989), The influence of sea-surface temperature on surface wind in the eastern equatorial Pacific: Weekly to monthly variability. Journal of Climate, 2, 1500–1506. doi:10.1175/1520-0442(1989)002%3C1500:TIOSST%3E2.0.CO;2

Hughes, P.J. (2016), The influence of small-scale sea surface temperature gradients on surface vector winds and subsequent impacts on oceanic Ekman pumping.

Jury, M. R. (1994), A thermal front within the marine atmospheric boundary layer over the Agulhas Current south of Africa: Composite aircraft observations. Journal of Geophysical Research, 99, 3297– 3304. doi:10.1029/93JC02400

——, & Walker, N. (1988), Marine boundary layer modification across the edge of the Agulhas Current. Journal of Geophysical Research, 93, 647–654. doi:10.1029/JC093iC01p00647

Moroni, D.F. (2008), A global and regional diagnostic comparison of air-sea flux parameterizations during episodic events.

Small, R. J., Xie, S. -P., & Wang, Y. (2003), Numerical simulation of atmospheric response to Pacific tropical instability waves. Journal of Climate, 16, 3723–3741. doi:10.1175/1520-0442(2003)016%3C3723:NSOART%3E2.0.CO;2

Small, R. J., deSzoeke, S. P., Xie, S. P., O'Neill, L., Seo, H., Song, Q., Cornillon, P., Spall, M., & Minobe, S. (2008), Air–sea interaction over ocean fronts and eddies. Dynamics of Atmospheres and Oceans, 45, 274–319, doi:10.1016/j.dynatmoce.2008.01.001.

Song, Q., Cornillon, P., & Hara, T. (2006), Surface wind response to oceanic fronts. Journal of Geophysical Research, 111, C12006, doi:10.1029/2006JC003680.

Spall, M. A. (2007), Midlatitude wind stress–sea surface temperature coupling in the vicinity of oceanic fronts. Journal of Climate, 20, 3785–3801. doi:10.1175/JCL14234.1.

Sweet, W. R., Fett, R., Kerling, J., & LaViolette, P. (1981), Ocean– atmosphere interaction effects in the lower troposphere across the north wall of the Gulf Stream. Monthly Weather Review, 109, 1042–1052. doi:10.1175/1520-0493(1981)109%3C1042:ASIEIT%3E2.0.CO;2

Tokinaga, H., Tanimoto, Y., & Xie, S. -P. (2005), SST-induced surface wind variations over the Brazil-Malvinas confluence: satellite and in situ observations. Journal of Climate, 18, 3470–3482. doi:10.1175/JCLI3485.1

Wallace, J. M., Mitchell, T. P., & Deser, C. (1989), The influence of sea surface temperature on surface wind in the eastern equatorial Pacific: Seasonal and interannual variability. Journal of Climate, 2, 1492–1499. doi:10.1175/1520-0442(1989)002%3C1492:TIOSST%3E2.0.CO;2